



Point-wise impulse (blast) response of a composite sandwich plate including core compressibility effects

Renfu Li, George A. Kardomateas *, George J. Simitse

Georgia Institute of Technology, School of Aerospace Engineering, Atlanta, GA 30332-0150, USA

ARTICLE INFO

Article history:

Received 24 April 2008

Received in revised form 27 October 2008

Available online 13 February 2009

Keywords:

Blast
Impulse
Impact
Compressibility
Sandwich
Composite
Plate
Non-linear

ABSTRACT

This work analyzes the nonlinear impulse response of a composite sandwich plate exposed to a sudden point-wise transverse loading on the top face sheet. The nonlinearity arising from the core compressibility in the thickness direction is modeled and incorporated into the constitutive relations explicitly. As such, one can have a deep insight regarding the stress, strain and displacement profiles into the sandwich plate. The sandwich plate is assumed to be perfectly bonded at the face sheet/core interfaces. The equations of motion are formulated using Hamilton's principle. The simply supported case is used to illustrate the procedure for solving the nonlinear equations. Numerical results are presented to demonstrate the response in terms of the transverse deformation and stresses in the composite sandwich plate. The effects of the variation of the geometrical parameters of the structure on the blast impulse response are also studied. Some conclusions are suggested regarding the associated optimal design of sandwich plates.

© 2009 Elsevier Ltd. All rights reserved.

1. Introduction

A typical sandwich plate consists of two stiff metallic or composite thin face sheets separated by a soft honeycomb or foam thick core of low density. This configuration gives the sandwich material system high stiffness and strength with little resultant weight penalty and high-energy absorption capability related to the application of sandwich structures in the construction of aerospace vehicles, naval vehicles and civil infrastructure. Most of the studies in sandwich composites neglect the transverse deformation of the core as mentioned in the Sandwich Structures books (Plantema, 1966; Allen, 1969; Vinson, 1999). The core of a sandwich structure is treated as infinitely rigid in the thickness direction and only its shear stresses are taken into account. This assumption works well in the analysis of sandwich structural response to a static or dynamic loading of long-duration. However, several studies (Kwon and Lannamann, 2002; Xue and Hutchinson, 2004; Fleck and Deshpande, 2004; Li et al., 2008) have shown that the core transverse deformation/strain in a sandwich structure subject to impulsive loading has a highly non-linear profile with respect to the thickness-wise coordinate. Although two models (Frostig et al., 1992; Librescu et al., 2004) consider transverse compressibility in the core, they yield either linear or constant transverse strain profiles.

It has been shown that the non-linear high order core theory in Li and Kardomateas (2008) is very accurate, yielding essentially identical results to the elasticity solution for static transverse loading. Therefore, this paper we shall extend this non-linear core model in to address the dynamic response of sandwich plates subject to point-wise blast impact loading. Consideration of the core compressibility implies that the displacements of the top and bottom face sheets may not be identical. The following assumptions will be adopted in this paper: (1) the face sheets satisfy the Kirchhoff-Love assumptions and their thicknesses are small compared with the overall thickness of the sandwich section, and the two face sheets are further assumed to have identical thickness; (2) the core is compressible in the transverse direction, that is, its thickness may change; (3) the bonding between the face sheets and the core is assumed perfect; and (4) an impulse loading decaying exponentially with time (blast loading) applied at a specific point on the top face of the plate will be considered.

This paper is organized as follows: the high order non-linear transverse compressible core theory assumptions are summarized in Section 2. The equations of motion and boundary and initial conditions are formulated in Section 3 via Hamilton's principle. These unknowns in the equations are highly coupled in terms of both the spatial and time variables. A solution procedure for solving the non-linear partial governing equations is formulated in Section 4 using the simply supported case as an example. Results from point-wise sudden impulse loading on the top face sheet of a sandwich plate are presented and discussed in Section 5. Suggested in Section 6 are some conclusions.

* Corresponding author. Tel.: +1 404 894 8198; fax: +1 404 894 9313.

E-mail address: george.kardomateas@aerospace.gatech.edu (G.A. Kardomateas).

2. Formulation

2.1. Kinematic relations

In the following, we consider a sandwich plate with two identical face sheets of thickness h_f and a core of thickness h_c and let a cartesian coordinate system (x, y, z) be on the middle plane of the core, as shown in Fig. 1. The corresponding displacements are denoted by (u, v, w) . We further use the superscript “ t, b, c ” to refer to the top face sheet, bottom face sheet or core, respectively, and the subscript “0” to refer to the middle surface of the corresponding phase.

The face sheets are assumed to satisfy the Kirchhoff-Love assumptions and their thicknesses are small compared with the overall thickness of the sandwich section. Therefore, if we define

$$\zeta = z \pm \left(\frac{h_c}{2} + \frac{h_f}{2} \right), \quad (1a)$$

in which the “ \pm ” sign in the variable ζ corresponds to the top and bottom face sheets respectively, the displacements for the top and bottom face sheets are expressed as:

$$u^{t,b}(x, y, z) = u_0^{t,b}(x, y) - \zeta w_x^{t,b}(x, y), \quad (1b)$$

$$v^{t,b}(x, y, z) = v_0^{t,b}(x, y) - \zeta w_y^{t,b}(x, y), \quad (1c)$$

$$w^{t,b}(x, y, z) = w^{t,b}(x, y), \quad -\frac{h_f}{2} \leq \zeta \leq \frac{h_f}{2}. \quad (1d)$$

Omitting the superscripts t and b , the non-linear strain-displacement relations for the face-sheets can take the following form:

$$[\epsilon] = \begin{bmatrix} \epsilon_{xx} \\ \epsilon_{yy} \\ \gamma_{xy} \end{bmatrix} = [\epsilon^0] + \zeta[k] = \begin{bmatrix} \epsilon_x^0 + \zeta k_x \\ \epsilon_y^0 + \zeta k_y \\ \gamma_{xy}^0 + \zeta k_{xy} \end{bmatrix}, \quad (2a)$$

in which $[\epsilon^0]$ is the middle surface strain given by

$$[\epsilon^0] = \begin{bmatrix} \epsilon_x^0 \\ \epsilon_y^0 \\ \gamma_{xy}^0 \end{bmatrix} = \begin{bmatrix} u_{0,x} + \frac{1}{2} w_x^2 \\ v_{0,y} + \frac{1}{2} w_y^2 \\ u_{0,y} + v_{0,x} + w_x w_y \end{bmatrix}. \quad (2b)$$

Moreover, $[k]$ is the curvature

$$[k] = \begin{bmatrix} k_x \\ k_y \\ k_{xy} \end{bmatrix} = \begin{bmatrix} -w_{,xx} \\ -w_{,yy} \\ -2w_{,xy} \end{bmatrix}. \quad (2c)$$

During the impulsive loading process, the core may undergo a considerable reduction in thickness. In order to capture this core transverse compressibility, we use a higher order core theory as formulated by Li and Kardomateas (2008). In this theory, the transverse displacement in the core, w^c is of fourth order in the transverse direction z :

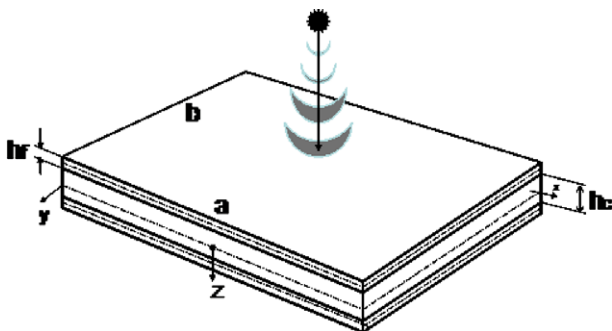


Fig. 1. A composite sandwich plate subject to point-wise blast (impulse) loading.

$$w^c(x, y, z) = \left(1 - \frac{2z^2}{h_c^2} - \frac{8z^4}{h_c^4} \right) w_0^c(x, y) + \left(\frac{2z^2}{h_c^2} + \frac{8z^4}{h_c^4} \right) \bar{w}(x, y) - \left(\frac{z}{h_c} + \frac{4z^3}{h_c^3} \right) \hat{w}(x, y), \quad -\frac{h_c}{2} \leq z \leq \frac{h_c}{2}, \quad (3a)$$

in which $w_0^c(x, y)$ is the transverse displacement of the middle surface of the core, and $\bar{w}(x, y)$ and $\hat{w}(x, y)$ are, respectively, the average and difference of the middle surface transverse displacements for the two face-sheets,

$$\bar{w}(x, y) = \frac{1}{2} [w^t(x, y) + w^b(x, y)],$$

$$\hat{w}(x, y) = \frac{1}{2} [w^t(x, y) - w^b(x, y)]. \quad (3b)$$

The in-plane displacements in the core, u^c and v^c , are of fifth order in z , expressed as follows:

$$u^c(x, y, z) = \bar{u}(x, y) - z \frac{2}{h_c} \hat{u}(x, y) + z \frac{h_f}{h_c} w_x^c(x, y, z), \quad (4a)$$

$$v^c(x, y, z) = \bar{v}(x, y) - z \frac{2}{h_c} \hat{v}(x, y) + z \frac{h_f}{h_c} w_y^c(x, y, z), \quad (4b)$$

where, $\bar{u}(x, y, t)$, $\hat{u}(x, y, t)$ and $\bar{v}(x, y, t)$, $\hat{v}(x, y, t)$ are, again, respectively, the average and difference of the middle surface in-plane displacements for the two face-sheets:

$$\bar{u}(x, y) = \frac{1}{2} [u_0^t(x, y) + u_0^b(x, y)],$$

$$\hat{u}(x, y) = \frac{1}{2} [u_0^t(x, y) - u_0^b(x, y)], \quad (4c)$$

$$\bar{v}(x, y) = \frac{1}{2} [v_0^t(x, y) + v_0^b(x, y)],$$

$$\hat{v}(x, y) = \frac{1}{2} [v_0^t(x, y) - v_0^b(x, y)]. \quad (4d)$$

These displacement profiles satisfy the displacement continuity, at the top face sheet/core interface, $z = -h_c/2$ and at the bottom face sheet/core interface, $z = h_c/2$.

It should be noted that like any other plate theory, this is still an approximate model and, although the displacement field satisfies all continuity and compatibility conditions, the equilibrium equations may not be satisfied within the core. However, a validation study for the static loading case has shown that this high order theory gives a displacement distribution almost exactly as the elasticity solution and a transverse stress distribution most close to the elasticity solution among all current sandwich theories (Li and Kardomateas, 2008).

The displacement profiles postulated above lead to the following strain relations for the core:

$$\epsilon_{zz}^c = \left(-\frac{1}{2h_c} + \frac{2z}{h_c^2} - \frac{6z^2}{h_c^3} + \frac{16z^3}{h_c^4} \right) w^t(x, y) - \left(\frac{4z}{h_c^2} + \frac{32z^3}{h_c^4} \right) w_0^c(x, y) + \left(\frac{1}{2h_c} + \frac{2z}{h_c^2} + \frac{6z^2}{h_c^3} + \frac{16z^3}{h_c^4} \right) w^b(x, y), \quad (5a)$$

$$\gamma_{xz}^c = -\frac{2}{h_c} \hat{u}(x, y) + \eta_1(z) w_x^t(x, y) + \eta_2(z) w_{0,x}^c(x, y) + \eta_3(z) w_x^b(x, y), \quad (5b)$$

$$\gamma_{yz}^c = -\frac{2}{h_c} \hat{v}(x, y) + \eta_1(z) w_y^t(x, y) + \eta_2(z) w_{0,y}^c(x, y) + \eta_3(z) w_y^b(x, y), \quad (5c)$$

in which,

$$\eta_1(z) = -\left(1 + \frac{2h_f}{h_c}\right) \frac{z}{2h_c} + \left(1 + \frac{3h_f}{h_c}\right) \frac{z^2}{h_c^2} - \left(1 + \frac{4h_f}{h_c}\right) \frac{2z^3}{h_c^3} + \left(1 + \frac{5h_f}{h_c}\right) \frac{4z^4}{h_c^4}, \quad (5d)$$

$$\eta_2(z) = \left(1 + \frac{h_f}{h_c}\right) - \left(1 + \frac{3h_f}{h_c}\right) \frac{2z^2}{h_c^2} - \left(1 + \frac{5h_f}{h_c}\right) \frac{8z^4}{h_c^4}, \quad (5e)$$

$$\eta_3(z) = \left(1 + \frac{2h_f}{h_c}\right) \frac{z}{2h_c} + \left(1 + \frac{3h_f}{h_c}\right) \frac{z^2}{h_c^2} + \left(1 + \frac{4h_f}{h_c}\right) \frac{2z^3}{h_c^3} + \left(1 + \frac{5h_f}{h_c}\right) \frac{4z^4}{h_c^4}. \quad (5f)$$

It should be noted that the core is considered undergoing large rotation with a small displacement, therefore, the in-plane strains can be neglected.

2.2. Constitutive relations

The equations developed so far can be applied to general materials. In the following sections, we will assume the face sheets are made of orthotropic laminated composites and the core is also orthotropic.

The general stress–strain relationship for any layer of the face sheets reads as:

$$\begin{bmatrix} \sigma_{xx} \\ \sigma_{yy} \\ \tau_{xy} \end{bmatrix} = \begin{bmatrix} C_{11} & C_{12} & C_{16} \\ C_{12} & C_{22} & C_{26} \\ C_{16} & C_{26} & C_{66} \end{bmatrix} \begin{bmatrix} \epsilon_{xx} \\ \epsilon_{yy} \\ \gamma_{xy} \end{bmatrix} \quad \text{or} \quad [\sigma] = [C][\epsilon], \quad (6a)$$

where C_{ij} for $i, j = 1, 2, 6$ are the plane-stress reduced stiffness coefficients. Therefore, based on classic laminated composite theory, one can find the resultants for the top or bottom face sheet of a sandwich plate as:

$$\begin{bmatrix} N_x \\ N_y \\ N_{xy} \end{bmatrix} = \begin{bmatrix} A_{11} & A_{12} & A_{16} \\ A_{12} & A_{22} & A_{26} \\ A_{16} & A_{26} & A_{66} \end{bmatrix} \begin{bmatrix} \epsilon_x^0 \\ \epsilon_y^0 \\ \gamma_{xy}^0 \end{bmatrix} + \begin{bmatrix} B_{11} & B_{12} & B_{16} \\ B_{12} & B_{22} & B_{26} \\ B_{16} & B_{26} & B_{66} \end{bmatrix} \begin{bmatrix} k_x^0 \\ k_y^0 \\ k_{xy}^0 \end{bmatrix}, \quad (6b)$$

for the resultant force and

$$\begin{bmatrix} M_x \\ M_y \\ M_{xy} \end{bmatrix} = \begin{bmatrix} B_{11} & B_{12} & B_{16} \\ B_{12} & B_{22} & B_{26} \\ B_{16} & B_{26} & B_{66} \end{bmatrix} \begin{bmatrix} \epsilon_x^0 \\ \epsilon_y^0 \\ \gamma_{xy}^0 \end{bmatrix} + \begin{bmatrix} D_{11} & D_{12} & D_{16} \\ D_{12} & D_{22} & D_{26} \\ D_{16} & D_{26} & D_{66} \end{bmatrix} \begin{bmatrix} k_x^0 \\ k_y^0 \\ k_{xy}^0 \end{bmatrix}, \quad (6c)$$

for the resultant moment. The A (extensional), B (coupling) and D (bending) stiffness matrices are respectively defined as:

$$[A_{ij}, B_{ij}, D_{ij}] = \begin{cases} \int_c^{c+f} C_{ij} \times \{1, z, z^2\} dz, & \text{for top face} \\ \int_{-c-f}^{-c} C_{ij} \times \{1, z, z^2\} dz, & \text{for bottom face} \end{cases} \quad i, j = 1, 2, 6. \quad (6d)$$

The stress–strain relations for an orthotropic core can be written as:

$$\sigma_{zz}^c = E^c \epsilon_{zz}^c, \quad \tau_{xz}^c = C_{xz}^c \gamma_{xz}^c, \quad \tau_{yz}^c = C_{yz}^c \gamma_{yz}^c. \quad (7)$$

3. Equations of motion

The equations of motion and appropriate boundary conditions can be derived using the Hamilton's principle. The sandwich plate is subject to an impulsive transverse loading $q(x, y, t)$ on the top

face-sheet. Let the strain energy be denoted by U , the external potential by W and the kinetic energy by T , then the variational principle states:

$$\delta[T - (U - W)] = 0, \quad (8)$$

in which,

$$\begin{aligned} \delta T = & \int_0^t \int_{-b/2}^{b/2} \int_{-a/2}^{a/2} \left[\int_{-\frac{h_c}{2}}^{-\frac{h_c}{2}-h_f} \rho^f (\dot{u}^t \delta \dot{u}^t + \dot{v}^t \delta \dot{v}^t + \dot{w}^t \delta \dot{w}^t) dz \right. \\ & + \int_{-\frac{h_c}{2}}^{\frac{h_c}{2}} \rho^c (\dot{u}^c \delta \dot{u}^c + \dot{v}^c \delta \dot{v}^c + \dot{w}^c \delta \dot{w}^c) dz \\ & \left. + \int_{\frac{h_c}{2}}^{\frac{h_c}{2}+h_f} \rho^f (\dot{u}^b \delta \dot{u}^b + \dot{v}^b \delta \dot{v}^b + \dot{w}^b \delta \dot{w}^b) dz \right] dx dy dt, \quad (9a) \end{aligned}$$

$$\begin{aligned} \delta U = & \int_0^t \int_{-b/2}^{b/2} \int_{-a/2}^{a/2} \left[\int_{-\frac{h_c}{2}}^{-\frac{h_c}{2}-h_f} (\sigma_{xx}^t \delta \epsilon_{xx}^t + \sigma_{yy}^t \delta \epsilon_{yy}^t + \tau_{xy}^t \delta \gamma_{xy}^t) dz \right. \\ & + \int_{-\frac{h_c}{2}}^{\frac{h_c}{2}} (\sigma_{zz}^c \delta \epsilon_{zz}^c + \tau_{xz}^c \delta \gamma_{xz}^c + \tau_{yz}^c \delta \gamma_{yz}^c) dz \\ & \left. + \int_{\frac{h_c}{2}}^{\frac{h_c}{2}+h_f} (\sigma_{xx}^b \delta \epsilon_{xx}^b + \sigma_{yy}^b \delta \epsilon_{yy}^b + \tau_{xy}^b \delta \gamma_{xy}^b) dz \right] dx dy dt, \quad (9b) \end{aligned}$$

$$\delta W = \int_0^t \int_{-b/2}^{b/2} \int_{-a/2}^{a/2} q(x, y, t) \delta w^t dx dy dt, \quad (9c)$$

where ρ is the mass density. The superscript t in the above equations denotes the corresponding values for the top face sheet whereas t when appearing in the variable list of the functions refers to time. The equation of motion and the boundary conditions can be obtained by substituting the stress–strain relations (6a) and (7) and displacements (3) and (4) into Eqs. (9), then into (8) and employing integration by parts. This results in seven equations, three for each face sheet and one for the core. There are seven unknowns: $u_o^t, v_o^t, w_o^t, u_o^c, v_o^c, w_o^c$.

The resulting equations for the top face sheet are:

$$\begin{aligned} \delta u_o^t: & N_{x,x}^t + N_{xy,y}^t - \left(\rho^f h_f + \rho^c \frac{h_c}{3} \right) \ddot{u}_o^t - \rho^c \frac{h_c}{6} \ddot{u}_o^b \\ & + \rho^c \frac{h_c h_f}{420} (23 \ddot{w}_{,x}^t + 17 \ddot{w}_{,o,x}^c - 5 \ddot{w}_{,x}^b) \\ & - G_{xz}^c \left[\frac{1}{h_c} (u_o^t - u_o^b) - \frac{11}{15} w_{o,x}^c - \alpha_0 (w_{,x}^t + w_{,x}^b) \right] = 0, \quad (10a) \end{aligned}$$

$$\begin{aligned} \delta v_o^t: & N_{xy,x}^t + N_{y,y}^t - \left(\rho^f h_f + \rho^c \frac{h_c}{3} \right) \ddot{v}_o^t - \rho^c \frac{h_c}{6} \ddot{v}_o^b \\ & + \rho^c \frac{h_c h_f}{420} (23 \ddot{w}_{,y}^t + 17 \ddot{w}_{,o,y}^c - 5 \ddot{w}_{,y}^b) \\ & - G_{yz}^c \left[\frac{1}{h_c} (v_o^t - v_o^b) - \frac{11}{15} w_{o,y}^c - \alpha_0 (w_{,y}^t + w_{,y}^b) \right] = 0, \quad (10b) \end{aligned}$$

and

$$\begin{aligned} \delta w_o^t: & M_{x,xx}^t + 2M_{xy,xy}^t + M_{y,yy}^t + (N_x^t w_{,x}^t)_{,x} + (N_{xy}^t w_{,x}^t)_{,y} + (N_{yx}^t w_{,y}^t)_{,x} \\ & + (N_y^t w_{,y}^t)_{,y} - \left(\rho^t h_f + \frac{29}{315} \rho^c h_c \right) \ddot{w}^t - \rho^c \frac{37 h_c}{630} \left(\ddot{w}_o^c - \frac{11}{37} \ddot{w}^b \right) \\ & + \left(\frac{\partial^2}{\partial x^2} + \frac{\partial^2}{\partial y^2} \right) \left[\rho^c \frac{19 h_c h_f^2}{1155} \ddot{w}^t + \frac{\rho^c h_c h_f^2}{27720} (199 \ddot{w}_o^c - 61 \ddot{w}^b) \right] \\ & - \rho^c \frac{h_c h_f}{420} [23 (\ddot{u}_{o,x}^t + \ddot{v}_{o,y}^t) + 5 (\ddot{u}_{o,x}^b + \ddot{v}_{o,y}^b)] \\ & + \alpha_1 h_c (G_{xz}^c w_{,xx}^t + G_{yz}^c w_{,yy}^t) + \alpha_2 h_c (C_{xz}^c w_{o,xx}^c + G_{yz}^c w_{o,yy}^c) \end{aligned}$$

$$\begin{aligned}
 & -\alpha_3 h_c (G_{xz}^c w_{,xx}^b + G_{yz}^c w_{,yy}^b) - \alpha_0 [G_{xz}^c (u_{0,x}^t - u_{0,x}^b) \\
 & + G_{yz}^c (v_{0,y}^t - v_{0,y}^b)] - \frac{61 E^c}{21 h_c} \left(w^t - \frac{358}{305} w_0^c + \frac{53}{305} w^b \right) \\
 & + q(x, y, t) = 0, \tag{10c}
 \end{aligned}$$

in which α_i ($i = 1, \dots, 4$) are constants in terms of the ratio of face thickness and core thickness as follows:

$$\alpha_0 = \frac{2}{15} + \frac{h_f}{2h_c}; \quad \alpha_1 = \frac{29}{315} + \frac{373 h_f}{630 h_c} + \frac{247}{252} \left(\frac{h_f}{h_c} \right)^2, \tag{11a}$$

$$\begin{aligned}
 \alpha_2 &= \frac{37}{630} + \frac{37 h_f}{630 h_c} - \frac{383}{630} \left(\frac{h_f}{h_c} \right)^2; \\
 \alpha_3 &= \frac{11}{630} + \frac{11 h_f}{630 h_c} - \frac{23}{180} \left(\frac{h_f}{h_c} \right)^2. \tag{11b}
 \end{aligned}$$

The equation of motion for the compressible core is:

$$\begin{aligned}
 \delta w_0^c : & \alpha_4 h_c (G_{xz}^c w_{0,xx}^c + G_{yz}^c w_{0,yy}^c) + \alpha_2 h_c [G_{xz}^c (w_{,xx}^t + w_{,xx}^b) \\
 & + G_{yz}^c (w_{,yy}^t + w_{,yy}^b)] - \frac{194}{315} h_c \rho \ddot{w}_0^c - \frac{37 h_c}{630} \rho^c (\ddot{w}^t + \ddot{w}^b) \\
 & - \frac{17 h_f h_c}{420} \rho^c (\ddot{u}_{0,x}^t + \ddot{v}_{0,y}^t) + \frac{17 h_f h_c}{420} \rho^c (\ddot{u}_{0,x}^b + \ddot{v}_{0,y}^b) \\
 & + \frac{181 h_f^2 h_c}{6930} \rho^c \left(\frac{\partial^2}{\partial x^2} + \frac{\partial^2}{\partial y^2} \right) [\ddot{w}_0^c + \frac{199}{724} (\ddot{w}^t + \ddot{w}^b)] \\
 & - \frac{358 E^c}{105 h_c} (2w_0^c - w^t - w^b) - \frac{11}{15} G_{xz}^c (u_{0,x}^t - u_{0,x}^b) \\
 & - \frac{11}{15} G_{yz}^c (v_{0,y}^t - v_{0,y}^b) = 0 \tag{12}
 \end{aligned}$$

where,

$$\alpha_4 = \frac{194}{315} + \frac{194 h_f}{315 h_c} + \frac{383}{315} \left(\frac{h_f}{h_c} \right)^2. \tag{13}$$

A similar set of equations for the motion of the bottom face sheet can be derived, as follows:

$$\begin{aligned}
 \delta u_0^b : & N_{x,x}^b + N_{xy,y}^b - \left(\rho^f h_f + \rho^c \frac{h_c}{3} \right) \ddot{u}_0^b - \rho^c \frac{h_c}{6} \ddot{u}_0^t \\
 & - \rho^c \frac{h_c h_f}{420} (23\ddot{w}_x^b + 17\ddot{w}_{0,x}^c - 5\ddot{w}_x^t) \\
 & - G_{xz}^c \left[\frac{1}{h_c} (u_0^t - u_0^b) - \frac{11}{15} w_{0,x}^c - \alpha_0 (w_{,x}^t + w_{,x}^b) \right] = 0, \tag{14a}
 \end{aligned}$$

$$\begin{aligned}
 \delta v_0^b : & N_{xy,x}^b + N_{y,y}^b - \left(\rho^f h_f + \rho^c \frac{h_c}{3} \right) \ddot{v}_0^b - \rho^c \frac{h_c}{6} \ddot{v}_0^t \\
 & - \rho^c \frac{h_c h_f}{420} (23\ddot{w}_y^b + 17\ddot{w}_{0,y}^c - 5\ddot{w}_y^t) \\
 & - G_{yz}^c \left[\frac{1}{h_c} (v_0^t - v_0^b) - \frac{11}{15} w_{0,y}^c - \alpha_0 (w_{,y}^t + w_{,y}^b) \right] = 0, \tag{14b}
 \end{aligned}$$

and

$$\begin{aligned}
 \delta w_0^b : & M_{x,xx}^b + 2M_{xy,xy}^b + M_{y,yy}^b + (N_x^b w_{,x}^b)_{,x} + (N_{xy}^b w_{,x}^b)_{,y} + (N_{yx}^b w_{,y}^b)_{,x} \\
 & + (N_y^b w_{,y}^b)_{,y} - \left(\rho^f h_f + \frac{29}{315} \rho^c h_c \right) \ddot{w}^b - \rho^c \frac{37 h_c}{630} \left(\ddot{w}_0^c - \frac{11}{37} \ddot{w}^t \right) \\
 & + \left(\frac{\partial^2}{\partial x^2} + \frac{\partial^2}{\partial y^2} \right) \left[\rho^c \frac{19 h_c h_f^2}{1155} \ddot{w}^b + \frac{\rho^c h_c h_f^2}{27720} (199\ddot{w}_0^c - 61\ddot{w}^t) \right] \\
 & + \rho^c \frac{h_c h_f}{420} [23(\ddot{u}_{0,x}^b + \ddot{v}_{0,y}^b) + 5(\ddot{u}_{0,x}^t + \ddot{v}_{0,y}^t)] \\
 & + \alpha_1 h_c (G_{xz}^c w_{,xx}^b + G_{yz}^c w_{,yy}^b) + \alpha_2 h_c (G_{xz}^c w_{0,xx}^c + G_{yz}^c w_{0,yy}^c) \\
 & - \alpha_3 h_c (G_{xz}^c w_{,xx}^t + G_{yz}^c w_{,yy}^t) - \alpha_0 [G_{xz}^c (u_{0,x}^t - u_{0,x}^b) \\
 & + G_{yz}^c (v_{0,y}^t - v_{0,y}^b)] - \frac{61 E^c}{21 h_c} \left(w^b - \frac{358}{305} w_0^c + \frac{53}{305} w^t \right) = 0. \tag{14c}
 \end{aligned}$$

The corresponding boundary conditions at $x = 0$, a read as follows:

For the top face sheet:

$$u_0^t = \tilde{u}^t \quad \text{or} \quad N_x^t = \tilde{N}_x^t, \tag{15a}$$

$$v_0^t = \tilde{v}^t \quad \text{or} \quad N_{xy}^t = \tilde{N}_{xy}^t, \tag{15b}$$

$$\begin{aligned}
 w^t &= \tilde{w}^t \quad \text{or} \quad N_x^t w_{,x}^t + M_{x,x}^t + N_{xy}^t w_{,y}^t + 2M_{xy,x}^t \\
 & + G_{xz}^c [\alpha_0 (u_0^b - u_0^t) + \alpha_1 h_c w_{,x}^t + \alpha_2 h_c w_{0,x}^c - \alpha_3 h_c w_{,x}^b] = \tilde{Q}_x^t, \tag{15c}
 \end{aligned}$$

where \tilde{Q}_x^t is the resultant top face sheet shear, defined as the integral of τ_{xz} over the top face sheet, and

$$w_{,x}^t = \tilde{w}_{,x}^t \quad \text{or} \quad M_x^t = \tilde{M}_x^t. \tag{15d}$$

For the core:

$$w_0^c = \tilde{w}_0^c \quad \text{or} \quad \frac{11}{15} (u_0^b - u_0^t) + \alpha_2 h_c w_{,x}^t + \alpha_4 h_c w_{0,x}^c + \alpha_2 h_c w_{,x}^b = \tilde{Q}_c, \tag{16}$$

where \tilde{Q}_c is the resultant core shear divided by the core shear modulus, i.e. \tilde{Q}_c is defined as the integral of τ_{xz}/G_c over the core.

For the bottom face sheet:

$$u_0^b = \tilde{u}^b \quad \text{or} \quad N_x^b = \tilde{N}_x^b, \tag{17a}$$

$$v_0^b = \tilde{v}^b \quad \text{or} \quad N_{xy}^b = \tilde{N}_{xy}^b, \tag{17b}$$

$$\begin{aligned}
 w^b &= \tilde{w}^b \quad \text{or} \quad N_x^b w_{,x}^b + M_{x,x}^b + N_{xy}^b w_{,y}^b + 2M_{xy,x}^b \\
 & + G_{xz}^c [\alpha_0 (u_0^b - u_0^t) - \alpha_3 h_c w_{,x}^t + \alpha_2 h_c w_{0,x}^c + \alpha_1 h_c w_{,x}^b] = \tilde{Q}_x^b, \tag{17c}
 \end{aligned}$$

where again \tilde{Q}_x^b is the resultant bottom face sheet shear, defined as the integral of τ_{xz} over the bottom face sheet, and

$$w_{,x}^b = \tilde{w}_{,x}^b \quad \text{or} \quad M_x^b = \tilde{M}_x^b. \tag{17d}$$

The superscript \sim denotes the known external boundary values.

Similar equations can be written for $y = 0, b$.

Assuming the sandwich plate is made of orthotropic materials and substituting Eq. (2b) into (6b) and (6c) and then into Eq. (10), one can rewrite the non-linear governing equations for the top face sheet as:

$$\begin{aligned}
 A_{11}^t u_{0,xx}^t + A_{66}^t u_{0,yy}^t + (A_{12}^t + A_{66}^t) v_{0,xy}^t - \frac{G_{xz}^c}{h_c} (u_0^t - u_0^b) \\
 - \left(\rho^f h_f + \rho^c \frac{h_c}{3} \right) \ddot{u}_0^t - \rho^c \frac{h_c}{6} \ddot{u}_0^b + \rho^c \frac{h_f h_c}{420} (23\ddot{w}_x^t + 17\ddot{w}_{0,x}^c - 5\ddot{w}_x^b) \\
 + G_{xz}^c \left[\frac{11}{15} w_{0,x}^c + \alpha_0 (w_{,x}^t + w_{,x}^b) \right] = \hat{F}_1^t, \tag{18a}
 \end{aligned}$$

$$\begin{aligned}
 (A_{21}^t + A_{66}^t) u_{0,xy}^t + A_{66}^t v_{0,xx}^t + A_{22}^t v_{0,yy}^t - \frac{G_{yz}^c}{h_c} (v_0^t - v_0^b) \\
 - \left(\rho^f h_f + \rho^c \frac{h_c}{3} \right) \ddot{v}_0^t - \rho^c \frac{h_c}{6} \ddot{v}_0^b + \rho^c \frac{h_f h_c}{420} (23\ddot{w}_y^t + 17\ddot{w}_{0,y}^c - 5\ddot{w}_y^b) \\
 + G_{yz}^c \left[\frac{11}{15} w_{0,y}^c + \alpha_0 (w_{,y}^t + w_{,y}^b) \right] = \hat{F}_2^t, \tag{18b}
 \end{aligned}$$

in which the last terms in the left-hand side of these equations reflect the effects of the higher order core theory, and the second from last terms in the left-hand side can be viewed as the excitation produced by the transverse motion for the in-plane motion; furthermore, the F_1^t, F_2^t terms in the right-hand side represent the nonlinear terms, and these are:

$$\hat{F}_1^t = -A_{11}w_x^t w_{xx}^t - (A_{12} + A_{66})w_y^t w_{xy}^t - A_{66}w_x^t w_{yy}^t, \quad (18c)$$

$$\hat{F}_2^t = -(A_{21} + A_{66})w_x^t w_{xy}^t - A_{66}w_{xx}^t w_y^t - A_{22}w_y^t w_{yy}^t. \quad (18d)$$

Furthermore, the third equation is:

$$\begin{aligned} & D_{11}^t w_{xxxx}^t + 2(D_{12}^t + 2D_{66}^t)w_{xxyy}^t + D_{22}^t w_{yyyy}^t \\ & + \frac{61}{21} \frac{E^c}{h_c} \left(w^t - \frac{358}{305} w_o^c + \frac{53}{305} w^b \right) + \left(\rho^t h_f + \rho^c \frac{29h_c}{315} \right) \ddot{w}^t \\ & + \rho^c \frac{37h_c}{630} \left(\dot{w}_o^c - \frac{11}{37} \dot{w}^b \right) - \left(\frac{\partial^2}{\partial x^2} + \frac{\partial^2}{\partial y^2} \right) \left[\rho^c \frac{19h_f^2 h_c}{1155} \ddot{w}^t \right. \\ & + \left. \frac{\rho^c h_f^2 h_c}{27720} (199\ddot{w}_o^c - 61\ddot{w}^b) \right] - \alpha_1 h_c (G_{xz}^c w_{xx}^t + G_{yz}^c w_{yy}^t) \\ & - \alpha_2 h_c (G_{xz}^c w_{o,xx}^c + G_{yz}^c w_{o,yy}^c) + \alpha_3 h_c (G_{xz}^c w_{xx}^b + G_{yz}^c w_{yy}^b) \\ & + \rho^c \frac{h_f h_c}{420} [23(\ddot{u}_{o,x}^t + \ddot{v}_{o,y}^t) + 5(\ddot{u}_{o,x}^b + \ddot{v}_{o,y}^b)] + \alpha_0 [G_{xz}^c (u_{o,x}^t - u_{o,x}^b) \\ & + G_{yz}^c (v_{o,y}^t - v_{o,y}^b)] = \hat{F}_3^t, \end{aligned} \quad (18e)$$

in which the last term in the left-hand side reflects the effects of the higher order core theory, and the second from last term in the left-hand side can be viewed as the effect from the in-plane motion on the transverse motion and F_3^t in the right-hand side is the nonlinear terms, as follows:

$$\hat{F}_3^t = (N_x^t w_x^t)_x + (N_{xy}^t w_x^t)_y + (N_{yx}^t w_y^t)_x + (N_y^t w_y^t)_y. \quad (18f)$$

Similarly, one can also recast the equation for core as follows:

$$\begin{aligned} & \alpha_4 h_c (G_{xz}^c w_{o,xx}^c + G_{yz}^c w_{o,yy}^c) + \alpha_2 h_c [G_{xz}^c (w_{xx}^t + w_{xx}^b) + G_{yz}^c (w_{yy}^t + w_{yy}^b)] \\ & - \frac{194}{315} \rho^c h_c \ddot{w}_o^c - \frac{358}{105} \frac{E^c}{h_c} (2w_o^c - w^t - w^b) - \frac{37h_c}{630} \rho^c (\ddot{w}^t + \ddot{w}^b) \\ & + \frac{181h_f^2 h_c}{6930} \rho^c \left(\frac{\partial^2}{\partial x^2} + \frac{\partial^2}{\partial y^2} \right) \left[\ddot{w}_o^c + \frac{199}{724} (\ddot{w}^t + \ddot{w}^b) \right] \\ & - \frac{17h_f h_c}{420} \rho^c (\ddot{u}_{o,x}^t + \ddot{v}_{o,y}^t - \ddot{u}_{o,x}^b - \ddot{v}_{o,y}^b) - \frac{11}{15} G_{xz}^c (u_{o,x}^t - u_{o,x}^b) \\ & - \frac{11}{15} G_{yz}^c (v_{o,y}^t - v_{o,y}^b) = 0. \end{aligned} \quad (19)$$

Finally, for the bottom face sheet, the equations of motion become:

$$\begin{aligned} & A_{11}^b u_{o,xx}^b + A_{66}^b u_{o,yy}^b + (A_{12}^b + A_{66}^b) v_{o,xy}^b + \frac{G_{xz}^c}{h_c} (u_o^t - u_o^b) \\ & - \left(\rho^b h_f + \frac{h_c}{3} \rho^c \right) \ddot{u}_o^b - \rho^c \frac{h_c}{6} \ddot{u}_o^t - \rho^c \frac{h_f h_c}{420} (23\ddot{w}_x^b + 17\ddot{w}_{o,x}^c - 5\ddot{w}_x^t) \\ & - G_{xz}^c \left[\frac{11}{15} w_{o,x}^c + \alpha_0 (w_x^t + w_x^b) \right] = \hat{F}_1^b, \end{aligned} \quad (20a)$$

$$\begin{aligned} & (A_{21}^b + A_{66}^b) u_{o,xy}^b + A_{66}^b v_{o,xx}^b + A_{22}^b v_{o,yy}^b + \frac{G_{yz}^c}{h_c} (v_o^t - v_o^b) \\ & - \left(\rho^b h_f + \frac{h_c}{3} \rho^c \right) \ddot{v}_o^b - \rho^c \frac{h_c}{6} \ddot{v}_o^t + \rho^c \frac{h_f h_c}{420} (5\ddot{w}_y^t - 17\ddot{w}_{o,y}^c - 23\ddot{w}_y^b) \\ & - G_{yz}^c \left[\frac{11}{15} w_{o,y}^c + \alpha_0 (w_y^t + w_y^b) \right] = \hat{F}_2^b, \end{aligned} \quad (20b)$$

and

$$\begin{aligned} & D_{11}^b w_{xxxx}^b + 2(D_{12}^b + 2D_{66}^b)w_{xxyy}^b + D_{22}^b w_{yyyy}^b \\ & + \frac{61}{21} \frac{E^c}{h_c} \left(\frac{53}{305} w^t - \frac{358}{305} w_o^c + w^b \right) - \left(\rho^b h_f + \rho^c \frac{29h_c}{315} \right) \ddot{w}^b \\ & + \rho^c \frac{37h_c}{630} \left(\dot{w}_o^c - \frac{11}{37} \dot{w}^t \right) - \left(\frac{\partial^2}{\partial x^2} + \frac{\partial^2}{\partial y^2} \right) \left[\rho^c \frac{19h_f^2 h_c}{1155} \ddot{w}^b \right. \end{aligned}$$

$$\begin{aligned} & \left. + \rho^c \frac{h_f^2 h_c}{27720} (199\ddot{w}_o^c - 61\ddot{w}^t) \right] + \alpha_3 h_c (G_{xz}^c w_{xx}^t + G_{yz}^c w_{yy}^t) \\ & - \alpha_2 h_c (G_{xz}^c w_{o,xx}^c + G_{yz}^c w_{o,yy}^c) - \alpha_1 h_c (G_{xz}^c w_{xx}^b + G_{yz}^c w_{yy}^b) \\ & - \rho^c \frac{h_f h_c}{420} [5(\ddot{u}_{o,x}^t + \ddot{v}_{o,y}^t) + 23(\ddot{u}_{o,x}^b + \ddot{v}_{o,y}^b)] + \alpha_0 [G_{xz}^c (u_{o,x}^t - u_{o,x}^b) \\ & + G_{yz}^c (v_{o,y}^t - v_{o,y}^b)] = \hat{F}_3^b, \end{aligned} \quad (20c)$$

in which the right-hand sides are the nonlinear terms:

$$\hat{F}_1^b = -A_{11}^b w_x^b w_{xx}^b - (A_{12}^b + A_{66}^b)w_y^b w_{xy}^b - A_{66}^b w_x^b w_{yy}^b, \quad (20d)$$

$$\hat{F}_2^b = -(A_{21}^b + A_{66}^b)w_x^b w_{xy}^b - A_{66}^b w_{xx}^b w_y^b - A_{22}^b w_y^b w_{yy}^b, \quad (20e)$$

$$\hat{F}_3^b = (N_x^b w_x^b)_x + (N_{xy}^b w_x^b)_y + (N_{yx}^b w_y^b)_x + (N_y^b w_y^b)_y. \quad (20f)$$

4. Solution procedure

In this section the solution procedure for the dynamic response of sandwich plates will be demonstrated through the study of the simply supported case. The boundary conditions along the $x = 0, a$ and $y = 0, b$ sides (Fig. 1) read as:

$$u_o^t = 0, \quad u_o^b = 0; \quad v_o^t = 0, \quad v_o^b = 0; \quad w^t = 0, \quad w^c = 0, \quad w^b = 0 \quad (21a)$$

and

$$M_{xx}^t = 0, \quad M_{xx}^b = 0 \quad \text{for } x = 0, a, \quad (21b)$$

$$M_{yy}^t = 0, \quad M_{yy}^b = 0 \quad \text{for } y = 0, b. \quad (21c)$$

The displacements can be assumed as:

$$\begin{aligned} u_o^t &= \sum_{m,n} U_{mn}^t(t) \cos \frac{m\pi x}{a} \sin \frac{n\pi y}{b}, \\ v_o^t &= \sum_{m,n} V_{mn}^t(t) \sin \frac{m\pi x}{a} \cos \frac{n\pi y}{b}, \end{aligned} \quad (22a)$$

$$\begin{aligned} u_o^b &= \sum_{m,n} U_{mn}^b(t) \cos \frac{m\pi x}{a} \sin \frac{n\pi y}{b}, \\ v_o^b &= \sum_{m,n} V_{mn}^b(t) \sin \frac{m\pi x}{a} \cos \frac{n\pi y}{b}, \end{aligned} \quad (22b)$$

$$\begin{aligned} w^t &= \sum_{m,n} W_{mn}^t(t) \sin \frac{m\pi x}{a} \sin \frac{n\pi y}{b}, \\ w^b &= \sum_{m,n} W_{mn}^b(t) \sin \frac{m\pi x}{a} \sin \frac{n\pi y}{b}, \end{aligned} \quad (22c)$$

$$w_o^c = \sum_{m,n} W_{mn}^c(t) \sin \frac{m\pi x}{a} \sin \frac{n\pi y}{b}, \quad (22d)$$

where $U_{mn}^t(t)$, $V_{mn}^t(t)$, $U_{mn}^b(t)$, $V_{mn}^b(t)$, $W_{mn}^t(t)$, $W_{mn}^b(t)$, and $W_{mn}^c(t)$ are unknown functions of time t . These displacements satisfy the boundary conditions. Substituting the displacements (22) into the equations of motion (18)–(20), with \hat{F}_i^t , \hat{F}_i^b ($i = 1, 2, 3$) and $q(x, y, t)$ being expressed into the following form:

$$\begin{aligned} \hat{F}_1^{t,b} &= \sum_{mn} \hat{F}_{1mn}^{t,b}(t) \cos \frac{m\pi x}{a} \sin \frac{n\pi y}{b}, \\ \hat{F}_2^{t,b} &= \sum_{mn} \hat{F}_{2mn}^{t,b}(t) \sin \frac{m\pi x}{a} \cos \frac{n\pi y}{b}, \end{aligned} \quad (23a)$$

$$\begin{aligned} \hat{F}_3^{t,b} &= \sum_{mn} \hat{F}_{3mn}^{t,b}(t) \sin \frac{m\pi x}{a} \sin \frac{n\pi y}{b}, \\ q(x,y,t) &= \sum_{mn} \hat{Q}_{mn}(t) \sin \frac{m\pi x}{a} \sin \frac{n\pi y}{b}, \end{aligned} \quad (23b)$$

we can obtain sets of second order ordinary differential equations with regard to the variable time in matrix form:

$$[M_{mn}]\ddot{U}_{mn}(t) + [\zeta_{mn}]\dot{U}_{mn}(t) + [\kappa_{mn}]U_{mn}(t) = F_{mn}(t), \quad (24)$$

where $[M_{mn}]$ is the equivalent mass matrix, $[\zeta_{mn}]$ is the damping coefficient matrix and $[\kappa_{mn}]$ is the equivalent spring constant matrix. These are 7×7 matrices for a given pair (m, n) .

The displacement vector U_{mn} is defined as $U_{mn} = [U_{mn}^t(t), V_{mn}^t(t), W_{mn}^t(t), W_{mn}^c(t), U_{mn}^b(t), V_{mn}^b(t), W_{mn}^b(t)]^T$ and the loading vector $F_{mn} = [\hat{F}_{1mn}^t(t) + \hat{Q}_{mn}(t), \hat{F}_{2mn}^t(t), \hat{F}_{3mn}^t(t), 0, \hat{F}_{1mn}^b(t), \hat{F}_{2mn}^b(t), \hat{F}_{3mn}^b(t)]^T$. The $\hat{F}_{jmn}^t(t), \hat{F}_{jmn}^b(t), \hat{Q}_{mn}(t)$ are obtained from Eqs. (23) as:

$$\hat{Q}_{mn}(t) = \frac{4}{ab} \int_0^a \int_0^b q(x,y,t) \sin \frac{m\pi x}{a} \sin \frac{n\pi y}{b}, \quad (25a)$$

$$\hat{F}_{1mn}^{t,b}(t) = \frac{4}{ab} \int_0^a \int_0^b \hat{F}_1^t \cos \frac{m\pi x}{a} \sin \frac{n\pi y}{b}, \quad (25b)$$

with similar expressions for the rest of the $\hat{F}_{jmn}^t(t)$ and $\hat{F}_{jmn}^b(t)$.

Next, applying the Laplace transform:

$$\tilde{U}(s) = L[U(t)](s) = \int_0^\infty U(t)e^{-st} dt \quad (26)$$

to Eq. (24), one can further obtain:

$$(s^2[M_{mn}] + s[\zeta_{mn}] + [\kappa_{mn}])\tilde{U}_{mn}(s) = \tilde{F}_{mn}(s). \quad (27)$$

In the Laplace space, the solution in terms of the displacements to Eq. (27) can be obtained without much difficulty if the loading vector $\tilde{F}_{mn} = [\tilde{F}_{1mn}^t + \tilde{Q}_{mn}(s), \tilde{F}_{2mn}^t, \tilde{F}_{3mn}^t, 0, \tilde{F}_{1mn}^b, \tilde{F}_{2mn}^b, \tilde{F}_{3mn}^b]^T$ is constant, then (27) is a set of linear algebraic equations, which can be solved directly for $\tilde{U}_{mn} = [\tilde{U}_{mn}^t, \tilde{V}_{mn}^t, \tilde{W}_{mn}^t, \tilde{W}_{mn}^c, \tilde{U}_{mn}^b, \tilde{V}_{mn}^b, \tilde{W}_{mn}^b]^T$ and then the displacements in time domain $U_{mn} = [U_{mn}^t(t), V_{mn}^t(t), W_{mn}^t(t), W_{mn}^c(t), U_{mn}^b(t), V_{mn}^b(t), W_{mn}^b(t)]^T$ can be recovered using the inverse Laplace Transform without much difficulty. Subsequently, the solution for the displacements can be found by using Eqs. (22). But the loading coefficients \tilde{F}_{jmn}^t and \tilde{F}_{jmn}^b were derived from the expressions (18c), (18d), (18f) and (20d)–(20f), which are non-linear functions of the displacements. Therefore, the right-hand side of (27), \tilde{F}_{mn} are non-linear functions of \tilde{U}_{mn} . Therefore, an iterative procedure is developed as follows: (1) First, \tilde{Q}_{mn} is a known function once the applied load is given. If the right-hand side of Eq. (27) is approximated by $\tilde{F}_{mn} = [\tilde{Q}_{mn}, 0, 0, 0, 0, 0, 0]^T$, then a first approximation to the solution is easily obtained as $\{\tilde{U}_{mn}(s) = s^{-2}[M_{mn}] + s[\zeta_{mn}] + [\kappa_{mn}]\}^{-1}\tilde{F}_{mn}$ (the superscript -1 denotes matrix inversion). (2) Application of the Inverse Laplace Transform to $\tilde{U}_{mn}(s)$ can lead to the corresponding solution $U_{mn}(t)$. Then, making use of Eqs. (18c), (18d), (18f), (20d)–(20f) and (22), one can determine the functions $\hat{F}_1^t, \hat{F}_2^t, \hat{F}_3^t$ and $\hat{F}_1^b, \hat{F}_2^b, \hat{F}_3^b$ and then the corresponding to these Laplace Transforms $\tilde{F}_1^t, \tilde{F}_2^t, \tilde{F}_3^t$ and $\tilde{F}_1^b, \tilde{F}_2^b, \tilde{F}_3^b$. (3) The next approximation for the displacements is found by solving Eq. (27) with the updated vector $\tilde{F}_{mn} = [\tilde{F}_{1mn}^t + \tilde{Q}_{mn}(s), \tilde{F}_{2mn}^t, \tilde{F}_{3mn}^t, 0, \tilde{F}_{1mn}^b, \tilde{F}_{2mn}^b, \tilde{F}_{3mn}^b]^T$. This procedure continues until the in-plane and transverse displacements are determined by the n th iteration with a convergence tolerance ϵ applied on the displacements normalized by the total height of the sandwich section, such that $\epsilon \leq 10^{-5}$ between two consecutive steps.

It should be mentioned that, in general, an iterative procedure combined with the Laplace transform in time to solve a set of non-linear equations, may converge or diverge depending on the coefficient matrices and the applied loading amplitudes. For practical structural configurations, the displacement solution is expected to converge until the dynamic buckling phenomenon occurs. In this study, in which we produce results for a realistic sandwich structure, we found that the solution is convergent after only six iterations.

5. Numerical results and discussions

In this section, we shall present the numerical results for typical sandwich plates with orthotropic phases. Since the sandwich structure consist of orthotropic phases, the relationship for the Poisson's ratios as: $\nu_{ij} = \nu_{ji}E_i/E_j$ will be applied without explicit explanation. Let us first consider faces with elastic constants (in GPa): $E_1^f = 40.0, E_2^f = 10.0, E_3^f = 10.0, G_{12}^f = 4.5, G_{23}^f = 3.5, G_{31}^f = 4.5$; Poisson's ratios: $\nu_{12}^f = 0.065, \nu_{31}^f = 0.260, \nu_{23}^f = 0.400$ (these are typical of glass/epoxy composite). The orthotropic core has elastic constants reading as (in GPa): $E_1^c = E_2^c = 0.032, E_3^c = E_z^c = 0.30, G_{12}^c = 0.013, G_{31}^c = 0.048, G_{23}^c = 0.048$; Poisson's ratios: $\nu_{12}^c = \nu_{31}^c = \nu_{32}^c = 0.25$ (these are typical of honeycomb material).

In the following we denote by h_{tot} the total thickness of the plate, defined as $h_{tot} = 2h_f + h_c$. In the example presented the face sheet thickness is $h_f = 2$ mm and the core thickness $h_c = 18$ mm. The plate dimensions are: $a = 25h_{tot}$ and $b = 50h_{tot}$. The top face of the sandwich plate is assumed to be blasted by a impulsive load at the point (x_0, y_0) , which is of the following form:

$$p(x,y) = p_0(t)\delta(x,x_0)\delta(y,y_0), \quad 0 < x, x_0 < a, \quad 0 < y, y_0 < b, \quad (28a)$$

where δ is the delta function. The intensity of the loading varies with time exponentially as

$$p_0(t) = Q_0 e^{-t/\alpha} \text{ MPa}, \quad t \geq 0, \quad (28b)$$

in which we use the values from Librescu et al. (2004): $Q_0 = 60.86$ and $\alpha = 3.33435$. From Eq. (25a) one can obtain the following loading in the transformed space:

$$Q_{mn} = \frac{4}{ab} p_0(t) \sin \frac{m\pi x_0}{a} \sin \frac{n\pi y_0}{b}, \quad 0 < x_0 < a, \quad 0 < y_0 < b. \quad (28c)$$

This loading case is the idealization of an explosive impact near a big sandwich plate. We shall study the case of $x_0 = 0.5a, y_0 = 0.5b$. However, all the methods and procedures can be extended for an arbitrary loading location of (x_0, y_0) .

Regarding the number of terms used in producing the results, we have used $m = 10$ and $n = 10$. No noteworthy difference in the results was found with a larger number of terms. In fact, we found that the calculations converge when $m \geq 8$ and $n \geq 8$, with no real difference beyond these levels of m and n .

Plotted in Fig. 2 is the distribution of the normalized transverse displacement as functions of y at $x = 0.5a$ in the face sheets and middle plane of the core at time instants $t = 25 \mu s$ and $250 \mu s$, respectively. The results demonstrate the evolution of motion propagating outward from the center points when the point-wise blast loading impacts on the top face at its center. Since the energy is still added into the sandwich material system from $t = 25 \mu s$ and $t = 250 \mu s$, the maximum amplitudes of these displacements increase during the evolution. One can also apparently see that the transverse displacements in the top face, middle plane of the core and bottom face are not identical. This observation is in good agreement with those in Li et al. (2008). A three dimensional displacement distribution profile for the top face sheet is presented

in Fig. 3 for time instant $t = 0.45$ ms, or $450 \mu\text{s}$. As expected, the maximum displacement occurs at the center point where the loading is applied.

Fig. 4 depicts the transient displacements for 4 different points $(0.5a, 0.5b)$, $(0.25a, 0.5b)$, $(0.5a, 0.25b)$ and $(0.25a, 0.25b)$ in the top face. Since $a \neq b$, the curves for $(0.25a, 0.5b)$ and $(0.5a, 0.25b)$ are not identical. One can further see that the displacements for the points $(0.25a, 0.5b)$, $(0.5a, 0.25b)$ and $(0.25a, 0.25b)$ could be tangled when $t \leq 10$ ms (in the sense that the displacement of a

further away point can even exceed that of a closer point), but these displacements decrease as the distance from the center point increases for each time instant of $t > 10$ ms. However, the maximum displacement occurs at the center when $t = 2.25$ ms.

Presented in Figs. 5–7 are the stress profiles in the core at three locations: $(x = 0.5a, y = 0.5b)$, $(x = 0.375a, y = 0.375b)$ and $(x = 0.25a, y = 0.25b)$, respectively. These profiles are used to demonstrate the stress distribution in the core through the thickness direction and as a function of time. In these figures $z/h_c = 0.5$ is along the interface between the bottom face and the core, and $z/h_c = -0.5$ is the interface between the core and the top face sheet, on which the impulsive impact is exerted. Fig. 5 shows that the stress is always negative (compressive) at the top face/core

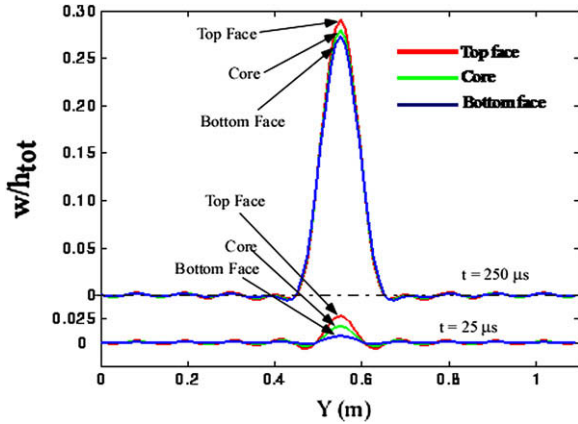


Fig. 2. Transverse displacements as a function of y for $x = 0.5a$ and at two time instants.

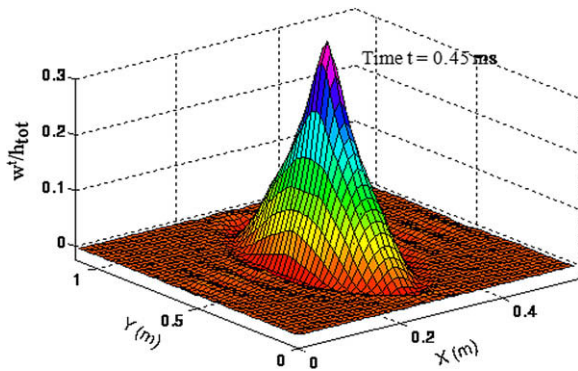


Fig. 3. Transverse displacement distribution at the top face sheet at $t = 0.45$ ms.

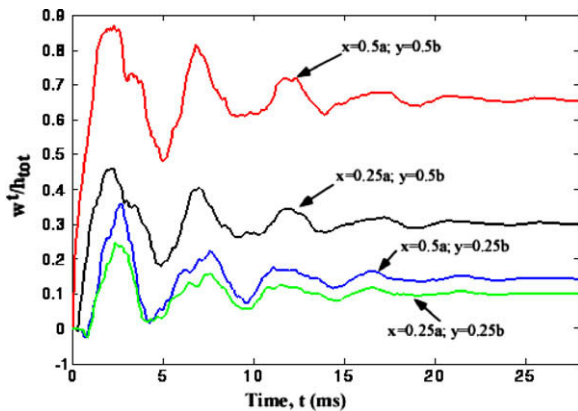


Fig. 4. Transverse displacement evolution with time at the top face sheet at different locations.

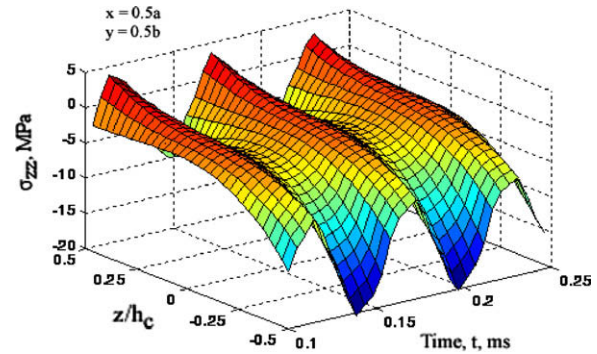


Fig. 5. Normal stress in the core at $x = 0.5a$ and $y = 0.5b$.

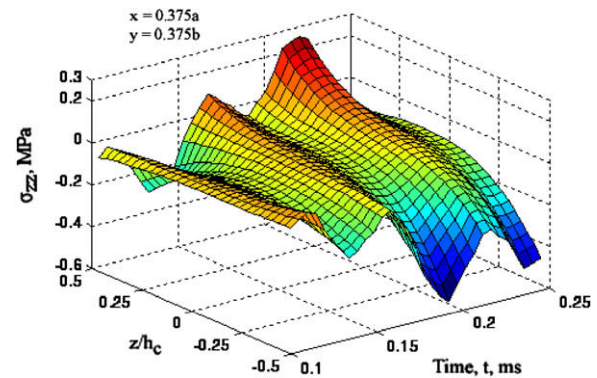


Fig. 6. Normal stress in the core at $x = 0.375a$ and $y = 0.375b$.

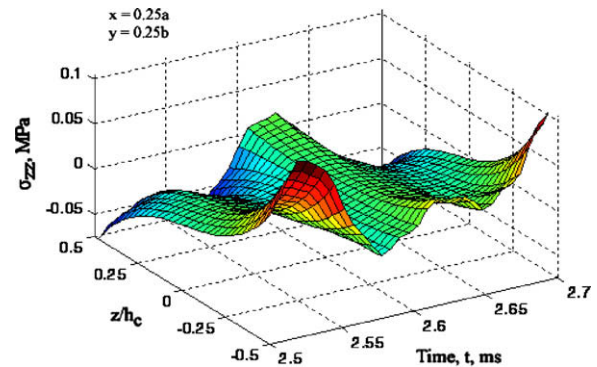


Fig. 7. Normal stress in the core at $x = 0.25a$ and $y = 0.25b$.

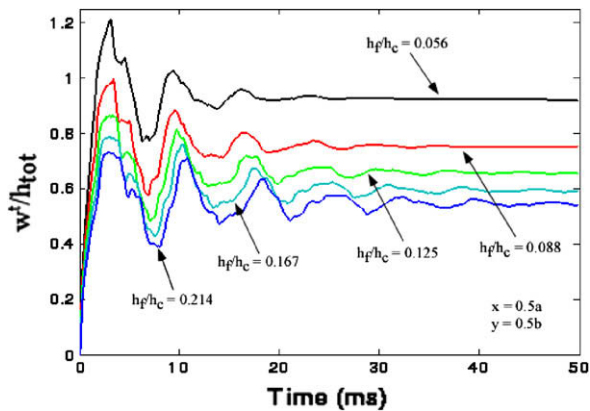


Fig. 8. Transverse displacement evolution with time at the top face sheet at $x = 0.5a$, $y = 0.5b$ and for various face sheet thicknesses (total plate thickness constant).

interface for $(x = 0.5a, y = 0.5b)$, but could be positive at the bottom face/core interface. One may also see that the maximum amplitude of the stress happens at the top face/core interface, as expected. These observations agree with the ones in Li et al. (2008), where the loading is uniformly distributed over the top face. However, at any position other than $(x = 0.5a, y = 0.5b)$, the stress could be either positive or negative at either of these interfaces, as shown in Figs. 6 and 7. One may also easily see that the maximum values in the transverse stress in the core of the sandwich plate decrease dramatically when x and y are away from $(0.5a, 0.5b)$.

The effects from the ratio of face sheet thickness over core thickness, h_f/h_c , on the transient response are illustrated in Fig. 8. In these results, the thickness of the plate is kept constant at 20mm. It can be seen that when h_f/h_c increases, the maximum value of the displacement at the center of the top face decreases. This observation has significance in the design of a sandwich structure. For example, if the maximum transverse deformation is the design criterion for certain sandwich structures, one must ensure the ratio h_f/h_c shall not be less than a critical value. In the meanwhile, this h_f/h_c may be as small as possible in order to ensure adequate weight savings. Therefore, the results can provide a guideline for optimal design.

6. Conclusions

The transient response of an orthotropic composite sandwich plate subject to point-wise impulse (blast) loading is studied using a nonlinear high order core theory. It is found that the top face, the core and the bottom face behave differently in the transient response. The transverse stress profiles in the core show high nonlinearity with maximum amplitudes at the interface between the core and top face sheet on which the blast loading impacts. Therefore, debonding could initiate at this interface as has been observed in preliminary experiments. The stress and displacement amplitudes decrease very rapidly away from the point loading. The effect of the ratio of face thickness over core thickness is analyzed and these observations could suggest some guidelines for sandwich plate optimal design.

Acknowledgments

The financial support of the Office of Naval Research, Grant N00014-07-10373, and the interest and encouragement of the Grant Monitor, Dr. Y.D.S. Rajapakse, are both gratefully acknowledged.

References

- Allen, H.G., 1969. Analysis and Design of Structural Sandwich Panels. Pergamon Press, Oxford.
- Fleck, N.A., Deshpande, V.S., 2004. The resistance of clamped sandwich beams to shock loading. *Journal of Applied Mechanics (ASME)* 71 (3), 386–401.
- Frostig, Y., Baruch, M., Vilnay, O., Sheinman, I., 1992. High-order theory for sandwich-beam behavior with transversely flexible core. *Journal of Engineering Mechanics* 118 (5), 1026–1043.
- Kwon, Y.W., Lannamann, D.L., 2002. Dynamic numerical modeling and simulation of interfacial cracks in sandwich structures for damage detection. *Journal of Sandwich Structures and Materials* 4 (2), 175–199.
- Li, R., Kardomateas, G.A., 2008. A nonlinear high order core theory for sandwich plates with orthotropic phases. *AIAA Journal* 46 (11), 2926–2934.
- Librescu, L., Oh, S.Y., Hohe, J., 2004. Linear and non-linear dynamic response of sandwich panels to blast loading. *Composite Part B: Engineering* 35, 673–683.
- Li, R., Kardomateas, G.A., Simitis, G.J., 2008. Non-linear response of a shallow sandwich shell with compressible core to blast loading. *Journal of Applied Mechanics (ASME)* 75 (6), 061023-1–061023-10.
- Plantema, F.J., 1966. Sandwich Construction. Wiley, New York.
- Vinson, J.R., 1999. The Behavior of Sandwich Structures of Isotropic and Composite Materials. Technomic Publishing Company, Lancaster, PA.
- Xue, Z., Hutchinson, J.W., 2004. A comparative study of impulse-resistant metal sandwich plates. *International Journal of Impact Engineering* 30, 1283–1305.